Journal of Hazardous Materials 167 (2009) 664–668

Contents lists available at ScienceDirect

Journal of Hazardous Materials

journal homepage: www.elsevier.com/locate/jhazmat

Photodegradation of phenol on Y_2O_3 surface Synergism by semiconductors

C. Karunakaran*, R. Dhanalakshmi, P. Anilkumar

Department of Chemistry, Annamalai University, Annamalainagar 608002, Tamilnadu, India

ARTICLE INFO

Article history:
Received 2 November 2008
Received in revised form 8 January 2009
Accepted 9 January 2009
Available online 19 January 2009

Keywords:
Insulator
Semiconductor
Interparticle electron-transfer
Photocatalysis

ABSTRACT

Under UV light, phenol degrades on the surface of Y_2O_3, an insulator, and the degradation follows first-order kinetics, depends linearly on the light intensity and slows down with pH. The efficiency of degradation is higher with UV-C light than with UV-A light. While particulate anatase TiO_2, ZnO, ZnS, Fe_2O_3, CuO, CdO, and Nb_2O_5 individually photodegrade phenol, each semiconductor shows synergism when present along with Y_2O_3, indicating electron-transfer from phenol adsorbed on Y_2O_3 to the illuminated semiconductors.

1. Introduction

Band gap-illumination of semiconductors generates electron-hole pairs, electrons in the conduction band and holes in the valence band [1]. Some of these pairs diffuse to the surface of the crystal and involve in chemical reactions with the adsorbed electron donors and acceptors, leading to photocatalysis. The hole oxidizes the organics and the adsorbed oxygen molecule takes up the electron, yielding highly unstable superoxide radical, $O_2^{\bullet -}$ [2]. In the presence of water, $O_2^{\bullet -}$ in turn generates reactive species such as $HO^{\bullet}$, $HO_2^{\bullet}$, and H_2O_2, which also oxidize the organics. Water is adsorbed on the semiconductor surface, molecularly as well as dissociatively [3,4]. Hole-trapping by either the surface hydroxyl groups or the adsorbed water molecules results in short-lived $HO^{\bullet}$ radicals, which are the primary oxidizing agents [5–8]. Semiconductor-photocatalysis is of interest due to its application in environmental remediation. But what we report here for the first time is photoreaction on the surface of Y_2O_3, an insulator and optical ceramic, used for coating aluminum and silver mirrors. Y_2O_3 is a low-absorption material in the near UV (300 nm) to IR (11 μm) region and the widely studied phenol photodegradation is the reaction taken up for the investigation; the semiconductors so far reported as photocatalysts for phenol degradation are TiO_2 in different forms [9,10], dye-sensitized TiO_2 [11], metal-doped TiO_2 [10], MoO_3 [12], MoS_2 [13], Fe_2O_3 [9,14], CuO [9], ZnO [9], ZnS [9], SnO_2 [13], ZrO_2 [9,12], HgO [9], PbO [9], PbO_2 [9], $GdCoO_3$ [15], CdSe/TiO_2 [16], In_2O_3/TiO_2 [17], WO_3/WS_2 [18], and $PW_{12}O_{40}^{3-}$ [14]. Moreover, the present study shows that the degradation on Y_2O_3 is enhanced by semiconductors, an unusual synergism when a semiconductor is present along with an insulator. Interparticle charge-transfer between semiconductors is known; a couple of reports are on charge-transfer between two particulate semiconductors [19,20] and the rest deal with coupled semiconductors [21,22].

2. Experimental

2.1. Materials

Y_2O_3 (Sd fine), TiO_2 (Merck), ZnO (Merck), ZnS (Sd fine), Fe_2O_3 (Fischer), CdO (Chemco), CuO (Sd fine) and Nb_2O_5 (Sd fine) used were of analytical grade.

2.2. Photoreactors

The photodegradation was made in a multilamp photoreactor fitted with eight 8 W mercury lamps of wavelength 365 nm (Sankyo Denki, Japan), a highly polished anodized aluminum reflector and four cooling fans at the bottom to dissipate the generated heat. The reaction vessel was a borosilicate glass tube of 15 mm inner diameter and was placed at the centre of the photoreactor. The light intensity was varied by using eight or four or two lamps with the angle sustained by the adjacent lamps at the sample as 45°, 90° and 180°, respectively. The degradation was also studied in a

* Corresponding author. Tel.: +91 94 43481590; fax: +91 41 44238145.
E-mail address: karunakaranc@rediffmail.com (C. Karunakaran).

0304-3894/$ – see front matter © 2009 Elsevier B.V. All rights reserved.
doi:10.1016/j.jhazmat.2009.01.034

Table 1
Particle size and BET surface area (*S*).

Catalyst	Size (μm)	S ($m^2\ g^{-1}$)
Y_2O_3	0.27–9.00	10.97
TiO_2	2.6–27.6	14.68
ZnO	3.5–27.6	12.16
ZnS	0.115–2.60	7.67
Fe_2O_3	2.6–27.6	17.84
CuO	5.69–30.5	1.51
CdO	2.6–11.4	14.45
Nb_2O_5	0.22–0.43	1.94

micro-photoreactor fitted with a 6 W 254 nm low-pressure mercury lamp and a 6 W 365 nm mercury lamp. Quartz and borosilicate glass tubes were used for 254 and 365 nm lamps, respectively. The light intensity under each experimental condition was determined by ferrioxalate actinometry [23].

2.3. Method

The photodegradation was carried out with 25 and 10 mL of phenol solutions in the multilamp and micro-photoreactors, respectively. The solution was continuously purged with air, which effectively kept the added catalyst under suspension and at motion. The airflow rate was determined by soap bubble method. After illumination, the catalyst was recovered by centrifugation and the undegraded phenol was analyzed fluorimetrically, after 100–500-times stepwise dilution. The excitation and emission wavelengths were set at 259 and 300 nm, respectively. The fall in the phenol concentration for a finite time of illumination afforded the degradation rate and the results were reproducible to ±5%. A time lag of at least 15 min was provided prior to illumination to ensure pre-adsorption of phenol on the catalyst. The dissolved O_2 was measured using an Elico dissolved oxygen analyzer PE 135, the pH was read with a Systronics μ pH System 361, the UV–visible spectra were recorded using a UV-1650 Shimadzu spectrophotometer, the fluorescence was measured with an Elico SL 174 spectrofluorimeter and an Avatar 330FT-IR spectrometer was employed to record the infrared spectra. The diffuse reflectance spectra were obtained using a Shimadzu UV-2450 UV–visible spectrometer with $BaSO_4$ as reference. Pre-sonication was made with a Toshcon SW 2 ultrasonic bath (37 ± 3 kHz, 150 W).

3. Results and discussion

3.1. Catalysts characterization

The TiO_2 used is of anatase form; the X-ray diffraction pattern of the sample totally matches with the standard pattern of anatase (JCPDS 00-021-1272) and the rutile lines (00-034-0180 D) are absent (Siemens D-5000 XRD, Cu K_α X-ray, λ = 1.54 Å, scan: 5–60°, scan speed: 0.2° s^{-1}). The XRD of ZnO is that of the JCPDS pattern of zincite (00-005-0664 D; Bruker D8 XRD, CuK_α X-ray, λ = 1.5406 Å, scan: 5–70°, scan speed: 0.050° s^{-1}). The particle sizes, determined using particle sizer Horiba LA-910 or Malvern 3600E (focal length 100 mm, beam length 2.0 mm, wet (methanol) presentation), are listed in Table 1. Also presented in Table 1 are the determined BET surface areas of the oxides and sulfides.

3.2. Photodegradation on Y_2O_3

The effect of various reaction parameters like illumination time, phenol concentration, photon flux and pH on the photoreaction was investigated using the multilamp-photoreactor with mercury lamps of wavelength 365 nm. Spectrofluorimetric and UV–visible spectral studies show continuous removal of phenol under UV light with Y_2O_3 and complete removal on prolonged illumination (Figs. 1 and 2); the solution illuminated for 4 h neither shows absorption in the UV region nor exhibits fluorescence. There is no stripping of phenol due to purging of air. Further, the adsorption of phenol on Y_2O_3 is small (~0.2%) compared to its degradation (12% in 15 min; conditions as in Fig. 1 but with 5.0 mM phenol). Y_2O_3 exhibits sustainable photocatalytic activity. The recycled catalyst without any pretreatment displays identical photocatalytic efficiency. Determination of the degradation rates at different phenol concentrations shows linear increase of the degradation rate with phenol concentration revealing the first-order kinetics; in the absence of Y_2O_3 the degradation is small (Fig. 3). Fig. 4 shows the linear dependence of the degradation rate on the light intensity and the loss of phenol due to photolysis is small. The photodegradation at different pH, under the conditions as stated in Fig. 1 but with 5.0 mM phenol, reveals decrease of the degradation rate (0.77 to 0.22 μM s^{-1}) with pH (3.0 to 8.8); the pH of the solution was modified by the addition of alkali or acid and measured after allowing the added catalyst to attain equilibrium with the phenol solution. The degradation using a 6 W 365 nm mercury lamp and a 6 W 254 nm low-pressure mercury lamp separately in the micro-reactor under identical conditions reveals that UV-C light is more effective than UV-A light to degrade phenol; the photocatalytic efficiencies of degradation at 365 and 254 nm-illuminations

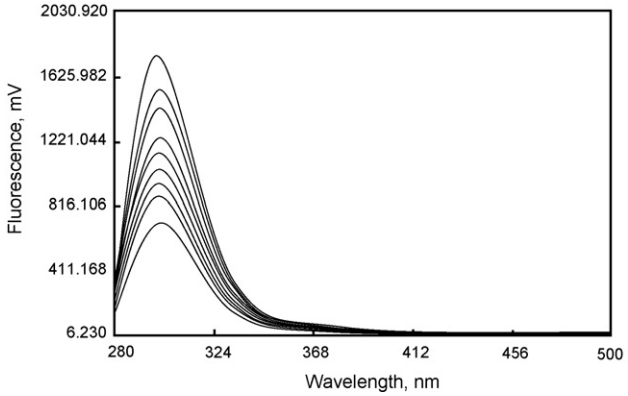

Fig. 1. The fluorescence spectra of illuminated phenol, 200-times diluted stepwise after the recovery of Y_2O_3, recorded at 0, 15, 30, 45, 60, 75, 90, 105, 120 min (↓); $[phenol]_0$ = 2.0 mM, Y_2O_3 loading = 0.10 g, airflow rate = 7.8 mL s^{-1}, $[O_2]_{dissolved}$ = 12.6 mg L^{-1}, phenol solution = 25 mL, λ = 365 nm, I = 25.4 μeinstein L^{-1} s^{-1}.

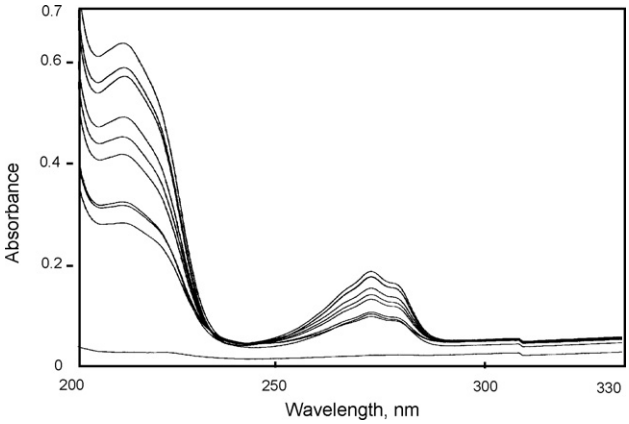

Fig. 2. The UV–vis spectra of illuminated phenol, 200-times diluted stepwise after the recovery of Y_2O_3, recorded at 0, 15, 30, 45, 60, 75, 90, 105, 120, 240 min (↓); $[phenol]_0$ = 2.0 mM, Y_2O_3 loading = 0.10 g, airflow rate = 7.8 mL s^{-1}, $[O_2]_{dissolved}$ = 12.6 mg L^{-1}, phenol solution = 25 mL, λ = 365 nm, I = 25.4 μeinstein L^{-1} s^{-1}.

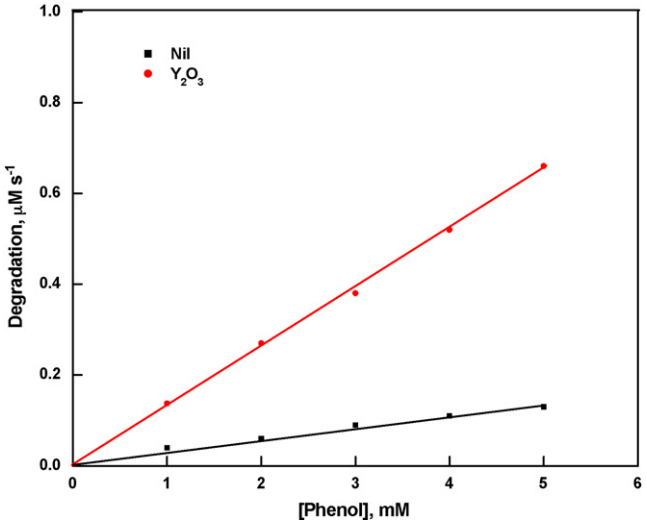

Fig. 3. Degradation as a function of phenol concentration; Y_2O_3 loading = 0.10 g, airflow rate = 7.8 mL s^{-1}, $[O_2]_{dissolved}$ = 12.6 mg L^{-1}, phenol solution = 25 mL, λ = 365 nm, I = 25.4 μeinstein L^{-1} s^{-1}, illumination = 15 min.

are 1.9% and 2.9%, respectively (10 mL 5.0 mM phenol, 0.10 g Y_2O_3 -loading, 7.8 mL s^{-1} airflow rate, 12.6 mL g^{-1} dissolved O_2). The photodegradation requires dissolved O_2. Deaeration of phenol solution by purging N_2 instead of air arrests the degradation (25 mL 5.0 mM phenol, 0.10 g Y_2O_3-loading, 25.4 μeinstein L^{-1} s^{-1} at 365 nm, 12.6 and 2.0 mg L^{-1} dissolved O_2 in air- and N_2-purged solutions, respectively). Singlet oxygen quencher azide ion (0.10 M) fails to inhibit the degradation pointing out the absence of the involvement of $^1O_2$ in the photodegradation. Vinyl monomer like acryl amide and acrylonitrile (5 mM) neither inhibits the photodegradation nor gets polymerized revealing the absence of chain carriers in the solution phase. Cationic as well as anionic micelles like cetyltrimethylammonium bromide, aerosol OT and sodium lauryl sulfate (5 mM) do not suppress the degradation suggesting that the rate of photodegradation is not governed by reaction in solution phase, if any. Generally, the photocatalytic efficiency is susceptible to the surface and size modification of the catalyst particles. Sonication in aqueous solution causes rapid formation, growth and collapse of cavities resulting in local high pressures and temperatures that are

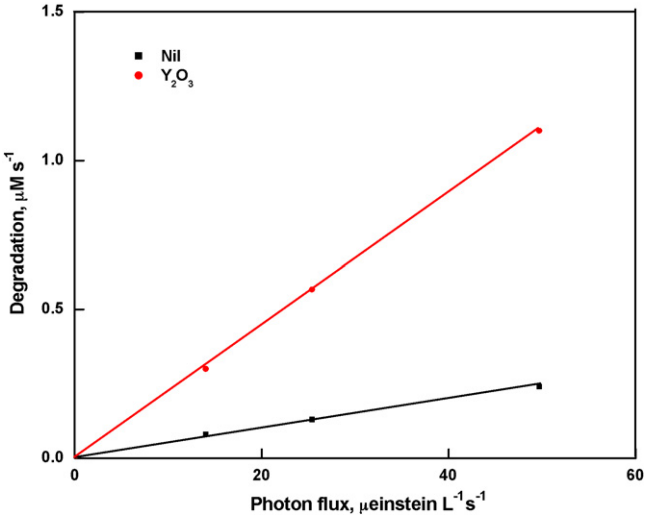

Fig. 4. Degradation as a function of photon flux; $[phenol]_0$ = 5.0 mM, Y_2O_3 loading = 0.10 g, $[O_2]_{dissolved}$ = 12.6 mg L^{-1}, phenol solution = 25 mL, λ = 365 nm, airflow rate = 7.8 mL s^{-1}, illumination = 15 min.

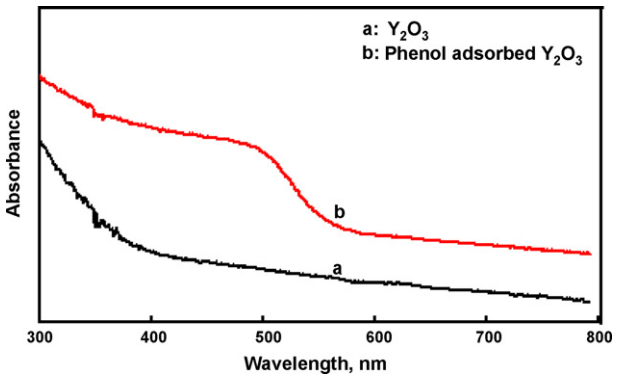

Fig. 5. Diffuse reflectance spectra of bare and phenol-adsorbed Y_2O_3 (a) bare Y_2O_3, (b) phenol-adsorbed Y_2O_3.

responsible for surface and particle size modification of the catalyst [24]. However, pre-sonication does not alter the photocatalytic efficiency; the rate of phenol degradation on Y_2O_3 is not significantly influenced by pre-sonication for 10 min at 37 ± 3 kHz and 150 W; for all the said experiments, the reaction conditions were as stated in Fig. 1 but with 5.0 nM phenol.

3.3. Mechanism

Water molecules get adsorbed over Y_2O_3 surface [25]. Analytical experiments show adsorption of phenol on Y_2O_3. The infrared spectrum of dried Y_2O_3, prior to illumination but after allowed to attain equilibrium with phenol solution, exhibits characteristic absorbance of aromatic –C=C– and of –OH group at ~630 and ~3420 cm^{-1}, respectively. On the surface of Y_2O_3, like that of Al_2O_3, besides the acidic and basic sites, hydroxyl groups are also present [25]. The acidic (Y^+) sites may coordinate with the phenolic oxygen and/or the basic O^- group may involve in hydrogen bonding with the –OH group of phenol. The slowdown of the photodegradation with increase of pH indicates that it is the molecular phenol but not the phenolate anion that gets adsorbed over Y_2O_3. The possible degradation mechanism is the light absorption by phenol adsorbed on Y_2O_3 surface leading to its excitation. The diffuse reflectance spectra of the phenol-adsorbed Y_2O_3 and bare Y_2O_3 confirm the same. While the absorption edge of phenol-adsorbed Y_2O_3 falls on the wavelength of illumination the bare Y_2O_3 does not absorb at the wavelength of illumination (Fig. 5). Transfer of the excited electron to an adjacent adsorbed oxygen molecule may initiate the phenol degradation. The report that 2,4,5-trichlorophenol forms a charge-transfer complex with TiO_2 which is activated by light of wavelength as long as 520 nm resulting in photochemical reaction supports the proposed mechanism [26]. The fact that the degradation does not occur in the absence of dissolved oxygen is in agreement with the proposition. The rest of the mechanism may be similar to that of semiconductor photocatalysis. A possible reason for the phenolate anion not getting adsorbed and photodegraded over Y_2O_3 surface is that it exists significantly in basic medium and the acidic sites on the oxide surface, which are required for its adsorption, cease to exist in basic solution. Further, the increase of pH favors the adsorption of hydroxide ion on the surface of Y_2O_3. Ion-dipole repulsion between the negatively charged oxide surface and the negative end of the phenolic -OH is possible. This may also be a factor for the decrease of the adsorption and hence the degradation of phenol on the oxide with increase of pH. A possible reason for the observed higher photonic efficiency with UV-C light than with UV-A light is the larger absorption of the former by Y_2O_3; the absorption edge of the oxide is close to the wavelength of the illuminated UV-C light [27].

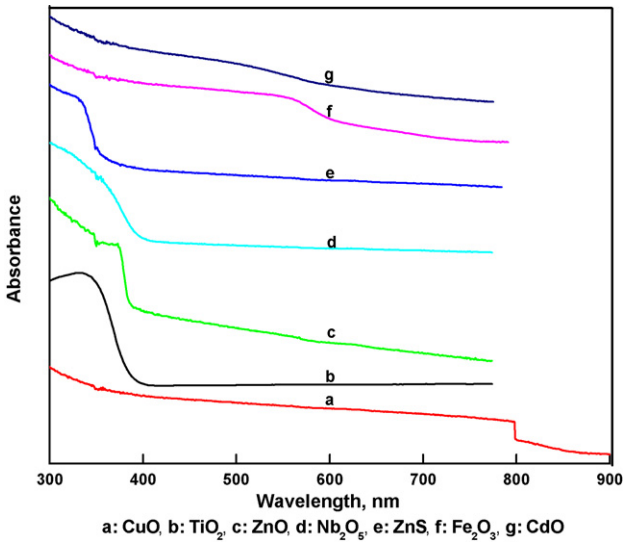

Fig. 6. Absorption edges of semiconductors.

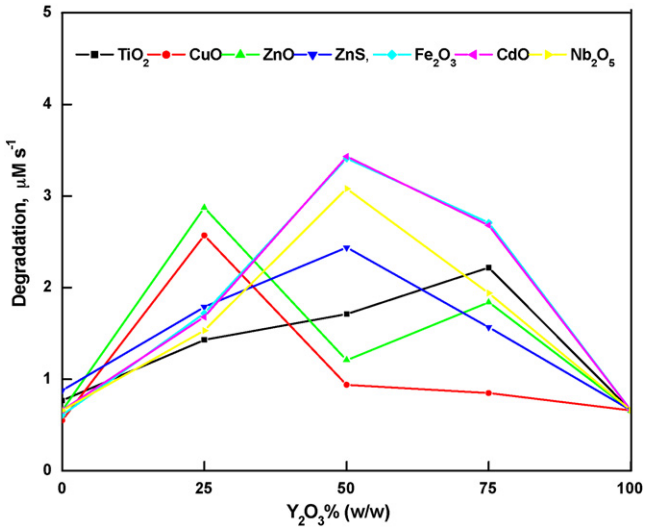

Fig. 7. Enhanced degradation by Y_2O_3 with semiconductors; $[phenol]_0 = 5.0$ mM, total catalyst loading = 0.10 g, airflow rate = 7.8 mL s^{-1}, $[O_2]_{dissolved} = 12.6$ mg L^{-1}, phenol solution = 25 mL, $\lambda = 365$ nm, $I = 25.4$ μeinstein L^{-1} s^{-1}.

3.4. Kinetic law

The Langmuir–Hinshelwood kinetic model is applicable to photodegradation and the corresponding law is [28]:

$$\text{rate} = \frac{kK_1K_2ICS[\text{phenol}][O_2]}{(1+K_1[\text{phenol}])(1+K_2[O_2])}$$

where K_1 and K_2 are the adsorption coefficients of phenol and molecular oxygen on the illuminated surface of Y_2O_3, k is the specific rate of degradation, S is the specific (BET) surface area of Y_2O_3, C is Y_2O_3-loading per litre and I is the light intensity in einstein L^{-1} s^{-1}. The phenol solution was oxygen-saturated by continuous purging of air and hence the dissolved oxygen concentration remained constant during the photodegradation. Since K_2 is constant $K_2[O_2]/(1+K_2[O_2])$ is also a constant. The Langmuir-Hinshelwood kinetic equation is valid for the observed results provided the adsorption coefficient of phenol on the illuminated surface of Y_2O_3 (K_1) is small so that $1 \gg K_1[\text{phenol}]$. This modifies the Langmuir-Hinshelwood equation to a linear dependence of the degradation rate on the phenol concentration. Although the adsorption of phenol on the surface of illuminated Y_2O_3 could not be measured, the analytical results in dark shows that Y_2O_3 adsorbs phenol at 5 mM to less than 0.2%.

3.5. Semiconductor photocatalysis

TiO_2, ZnO, ZnS, Fe_2O_3, CuO, CdO and Nb_2O_5 catalyze the degradation of phenol under UV light. All the stated semiconductors exhibit band gap-excitation at the wavelength of illumination and Fig. 6, the diffuse reflectance spectra, confirm the same. The determined rates of photodegradation of phenol on TiO_2, ZnO, ZnS, Fe_2O_3, CuO, CdO and Nb_2O_5 are 0.77, 0.66, 0.88, 0.61, 0.55, 0.66 and 0.66 μM s^{-1}, respectively (25 mL 5.0 mM phenol, 0.10 g catalyst-loading, 7.8 mL s^{-1} airflow rate, 12.6 mg L^{-1} dissolved O_2, 25.4 μeinstein L^{-1} s^{-1} at 365 nm).

3.6. Synergism by semiconductors

Band gap-excitation of semiconductors in a coupled system enables vectorial transfer of holes and excited electrons from one semiconductor to another leading to enhanced photocatalytic efficiency and increased photocatalysis by semiconductor mixtures is known [19,20]. But what we observe here is enhanced photocatalysis due to the presence of a particulate semiconductor with particulate Y_2O_3, both under suspension and at continuous motion due to purging of air in the illuminated solution; semiconductor was mixed and ground with Y_2O_3 and used as the photocatalyst. All the semiconductors used show the enhancement with Y_2O_3 (Fig. 7). This is due to electron-transfer from the phenol molecule adsorbed on Y_2O_3 to the illuminated semiconductor. The reason for not observing the maximum photocatalytic efficiency at 50% composition could be the non-uniformity of the particle sizes and also the densities of the catalysts.

4. Conclusions

Y_2O_3 mediates the degradation of phenol under UV light. The degradation depends on phenol concentration, photon flux and acidity of the solution. UV-C light is more effective than UV-A light to degrade phenol on Y_2O_3 surface. While semiconductors TiO_2, ZnO, ZnS, Fe_2O_3, CuO, CdO and Nb_2O_5 individually photocatalyze the degradation of phenol they show synergistic effect, an enhanced photocatalysis, when present along with Y_2O_3 indicating abstraction of electron from phenol molecule adsorbed on Y_2O_3 by the illuminated semiconductors.

Acknowledgements

The authors thank the Council of Scientific and Industrial Research (CSIR), New Delhi, for the financial support through research grant no. 01(2031)/06/EMR-II and R.D. is grateful to Annamalai University for UF.

References

[1] M.R. Hoffmann, S.T. Martin, W. Choi, D.W. Bahnemann, Environmental applications of semiconductor photocatalysis, Chem. Rev. 95 (1995) 69–96.
[2] T.L. Thompson, J.T. Yates Jr., Surface science studies of the photoactivation of TiO_2 – new photochemical process, Chem. Rev. 106 (2006) 4428–4453.
[3] R. Osgood, Photoreaction dynamics of molecular adsorbates on semiconductor and oxide surfaces, Chem. Rev. 106 (2006) 4379–4401.
[4] J. Zhao, B. Li, K. Onda, M. Feng, H. Petek, Solvated electrons on metal oxide surfaces, Chem. Rev. 106 (2006) 4402–4427.
[5] J. Peller, O. Wiest, P.V. Kamat, Hydroxy radical's role in the remediation of a common herbicide, 2,4-dichlorophenoxyacetic acid (2,4-D), J. Phys. Chem. A 108 (2004) 10925–10933.
[6] Y. Shiraishi, N. Saito, T. Hirai, Adsorption-driven photocatalytic activity of mesoporous titanium dioxide, J. Am. Chem. Soc. 127 (2005) 12820–12822.

[7] Y. Du, J. Rabani, The measure of TiO_2 photocatalytic efficiency and the comparison of different photocatalytic titania, J. Phys. Chem. B 107 (2003) 11970–11978.
[8] L. Sun, J.R. Bolton, Determination of the quantum yield for the photochemical generation of hydroxyl radicals in TiO_2 suspensions, J. Phys. Chem. 100 (1996) 4127–4134.
[9] C. Karunakaran, R. Dhanalakshmi, Semiconductor-catalyzed degradation of phenols with sunlight, Solar Energy Mater. Solar Cells 92 (2008) 1315–1321.
[10] C.A. Emilio, M.I. Litter, M. Kunst, M. Bouchard, C. Colbeau-Justin, Phenol photodegradation on platinized-TiO_2 photocatalysts related to charge-carrier dynamics, Langmuir 22 (2006) 3606–3613.
[11] V. Iliev, Phthalocyanine-modified titania-catalyst for photooxidation of phenols by irradiation with visible light, J. Photochem. Photobiol. A: Chem. 151 (2002) 195–199.
[12] G. Al-Sayyed, J.-C. D'Oliveira, P. Pichat, Semiconductor-sensitized photodegradation of 4-chlorophenol in water, J. Photochem. Photobiol. A: Chem. 58 (1991) 99–114.
[13] J.P. Wilcoxon, Catalytic photooxidation of pentachlorophenol using semiconductor nanoclusters, J. Phys. Chem. B 104 (2000) 7334–7343.
[14] M. Pera-Titus, V. Garcia-Molina, M.A. Banos, J. Gimenez, S. Esplugas, Degradation of chlorophenols by means of advanced oxidation processes: a general review, Appl. Catal. B: Environ. 47 (2004) 219–256.
[15] P. Mahata, T. Aarthi, G. Madras, S. Natarajan, Photocatalytic degradation of dyes and organics with nanosized $GdCoO_3$, J. Phys. Chem. C 111 (2007) 1665–1674.
[16] S.C. Lo, C.F. Lin, C.H. Wu, P.H. Hsieh, Capability of coupled CdSe/TiO_2 for photocatalytic degradation of 4-chlorophenol, J. Hazard. Mater. 114 (2004) 183–190.
[17] D.G. Shchukin, R.A. Caruso, Template synthesis and photocatalytic properties of porous metal oxide spheres formed by nanoparticle infiltration, Chem. Mater. 16 (2004) 2287–2292.
[18] A. Di Paola, L. Palmisano, V. Augugliaro, Photocatalytic behavior of mixed WO_3/WS_2 powders, Catal. Today 58 (2000) 141–149.
[19] N. Serpone, E. Borgarello, M. Gratzel, Visible light induced generation of hydrogen from H_2S in mixed semiconductor dispersions; improved efficiency through inter-particle electron transfer, J. Chem. Soc. Chem. Commun. (1984) 342–344.
[20] N. Serpone, P. Maruthamuthu, P. Pichat, E. Pelizzetti, H. Hidaka, Exploiting the interparticle electron transfer process in the photocatalyzed oxidation of phenol, 2-chlorophenol and pentachlorophenol: chemical evidence for electron and hole transfer between coupled semiconductors, J. Photochem. Photobiol. A: Chem. 85 (1995) 247–255.
[21] J. Bandara, K. Tennakone, P. Binduhewa, Probing the tunneling of electrons from SnO_2 to ZnO in dye sensitization of composite SnO_2/ZnO by use of generated H_2O_2 via reduction of O_2, New J. Chem. 25 (2001) 1302–1305.
[22] K.C. Kim, C.S. Han, Photocatalysis over titania on iron oxide, J. Phys. IV France 132 (2006) 185–188.
[23] H.J. Kuhn, S.E. Braslavsky, R. Schmidt, Chemical actinometry (IUPAC technical report), Pure Appl. Chem. 76 (2004) 2105–2146.
[24] K. Hirano, H. Nitta, K. Sawada, Effect of sonication on the photocatalytic mineralization of some chlorinated organic compounds, Ultrason. Sonochem. 12 (2005) 271–276.
[25] D.F. Bezuidenhout, R. Pretorius, The optical properties of evaporated Y_2O_3 films, Thin Solid Films 139 (1986) 121–132.
[26] A.G. Agrios, K.A. Gray, E. Weitz, Photocatalytic transformation of 2,4,5-trichlorophenol on TiO_2 under sub-band-gap illumination, Langmuir 19 (2003) 1402–1409.
[27] C. Sol, R.J.D. Tilley, Ultraviolet laser irradiation induced chemical reactions of some metal oxides, J. Mater. Chem. 11 (2001) 815–820.
[28] C. Karunakaran, S. Senthilvelan, S. Karuthapandian, TiO_2-photocatalyzed oxidation of aniline, J. Photochem. Photobiol. A: Chem. 172 (2005) 207–213.